Evolution of an Archean Metamorphic Belt: A Conventional and SHRIMP U-Pb Study of Accessory Minerals from the Jimperding Metamorphic Belt, Yilgarn Craton, West Australia

Delphine Bosch, Olivier Bruguier, Robert Pidgeon

Evolution of an Archean Metamorphic Belt: A Conventional and SHRIMP U-Pb Study of Accessory Minerals from the Jimperding Metamorphic Belt, Yilgarn Craton, West Australia[1]

Delphine Bosch, Olivier Bruguier, and Robert T. Pidgeon[2]

Laboratoire de Géochronologie-Géochimie-Pétrologie, Case courrier 066, CNRS-UMR 5567, Université de Montpellier II, Pl. E. Bataillon, 34095 MONTPELLIER Cedex 5, FRANCE

ABSTRACT

U-Pb TIMS analyses of zircon, monazite, titanite, and apatite combined with SHRIMP U-Th-Pb analyses of zircons from magmatic and metasedimentary rocks of the Jimperding Metamorphic Belt in the southwestern part of the Yilgarn craton (Western Australia), provide reliable information on the evolution of this belt. SHRIMP analyses on single detrital zircon grains suggest the sediments originated from Archean sources similar in age to the Narryer Gneiss Complex. Deposition of the clastic metasediments is bracketed by the youngest concordant grain (3055 ± 12 Ma) and the minimum age of a possible amphibolite dike crosscutting the sediments (2711 ± 7 Ma). SHRIMP and TIMS analyses on zircons from a porphyritic granite and an orthogneiss indicate that magmatism occurred during the prograde stage of a regional metamorphic event (2660–2670 Ma). Metamorphic monazites from pelitic schists define an age of 2661 ± 1 Ma that relates to mineral growth, also during the prograde stage of metamorphism. Peak metamorphism was reached at ca. 2650 Ma, as demonstrated by titanite from a deformed orthogneiss (2649 ± 4 Ma). This period is coeval with the production of granulitic facies assemblages farther east and with the age of magmatic zircons from the adjacent Katrine syenite. By combining age estimates for monazite growth in pelitic terranes with closure temperatures for other accessory minerals, the rates of thermal processes accompanying the late Archean regional metamorphism in the southwestern Yilgarn Craton can be assessed. During prograde metamorphism, the heating rate was ca. 15°C Ma^{-1} followed by a post-metamorphic cooling from approximately -10°C Ma^{-1} to $-1/-2$°C Ma^{-1}.

Introduction

Precise dating of single grain and part-grain samples of U-bearing accessory minerals has opened up new opportunities for determining the timing of igneous and metamorphic activity in complex terranes. Already there have been a number of case histories where these data have provided new insights into the timing and processes of an orogenic episode (Schärer et al. 1986; Corfu 1988), and a number of studies (e.g., Copeland et al. 1988; Smith and Barreiro 1990; Cherniak et al. 1991; Cherniak 1993) have been devoted to calibrating the behavior of key accessory minerals such as zircons, monazite, titanite, and apatite as temperature and petrological markers for metamorphic reactions, igneous crystallization, and regional cooling. The Jimperding Metamorphic Belt (JMB) (figure 1), in the Archean Yilgarn Craton of Western Australia provides a complex history of igneous and tectonic events and represents an ideal field laboratory for comparing and contrasting the isotopic behavior of mineral isotopic systems. In this study we investigated U-Pb systems of zircon, titanite, monazite, and apatite using conventional and SHRIMP techniques on samples from adjacent igneous and metamorphic rocks within an approximately 1 km^2 area in the central part of the belt near Toodyay (figure 2). The results provide general information on the behavior of mineral U-Pb systems and contribute to our understanding of the metamorphic and magmatic processes operating during late Archean tectonism in the southwest Yilgarn Craton.

[1] Manuscript received February 15, 1996; accepted June 6, 1996.

[2] School of Applied Geology, Curtin University of Technology, GPO Box U 1987, Perth 6001, Western Australia.

[Journal of Geology, 1996, volume 104, p. 695–711] 0022-1376/96/10406-0005$1.00

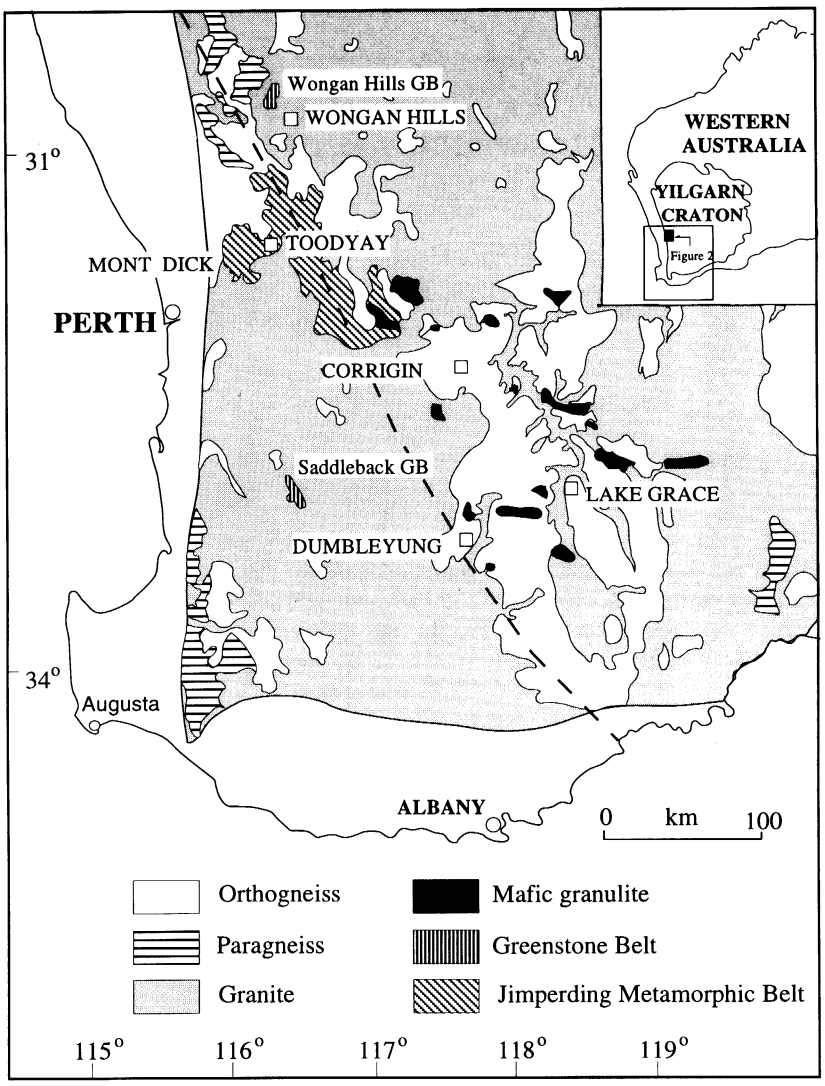

Figure 1. Geological map of the southwestern Yilgarn Craton of Western Australia. Location of figure 2 is shown in the box at the upper right-hand corner. Dashed line represents the major change in gravity.

Geological Background

General Presentation. The JMB lies in the southwestern Yilgarn Craton of Western Australia (figure 1). The rather limited geological knowledge of this part of the Craton has been summarized by Wilde (1980) and Gee et al. (1981). These authors describe the Jimperding belt as a NW-trending belt of ortho- and para-gneisses flanked and intruded by late Archean granitoids (figure 1). The belt consists of a complex folded series of quartzites, with rare cross-bedding, lenses of ultramafic rocks (presently cordierite-anthophyllite schist, talc rocks, and pyroxenite), lens-shaped bodies of amphibolite, sillimanite schists, and banded ironstone. The nature of the sequence suggests original estuarine sedimentation with material derived from a felsic hinterland followed by intrusion of basic, ultrabasic, and granite magmas. The geology of the belt is dominated by a Late Archean episode of high-grade metamorphism, deformation, and igneous intrusion. Intrusion by granitoids, prior to and after the deformation and metamorphism, is evidenced by comformable migmatites and gneisses and post-deformational granites, pegmatites, and aplites (Wilde and Low 1978). The belt is located on a major change in gravity (heavy dotted line in figure 1) that may represent a major structural feature marking the contact of two terranes (Fraser and Pettifer 1980). An eastward increase in metamorphic grade from lower amphibolite to granulite facies occurs across the belt (Wilde 1980), and the mineralogical assemblages of the rocks in the Katrine area, where the present samples were taken, suggests the metamorphic grade is close to the boundary between upper amphibolite and granulite facies.

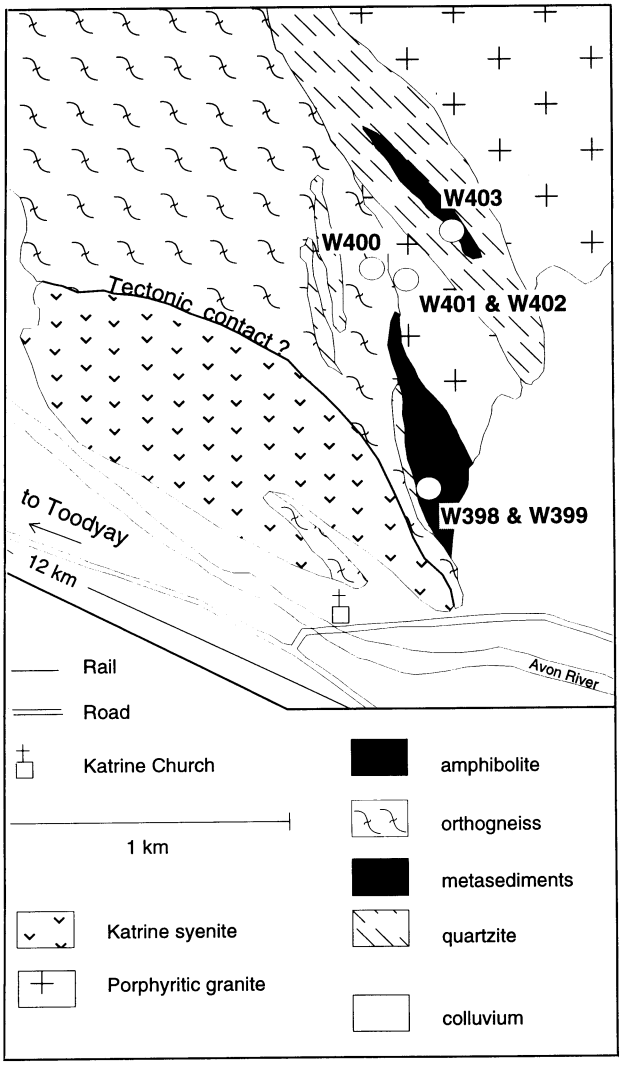

Figure 2. Map of the Toodyay area of the Jimperding Metamorphic Belt with location of the studied samples. W398: Pelitic Schist; W399: Psammopelite; W400; Orthogneiss; W401: Porphyritic Granite; W402: Schist (xenolith in W401); W403: Amphibolite.

Previous Geochronology. The presence of an older Archean provenance for the Jimperding belt has been demonstrated by SHRIMP analyses as detrital zircons from the Windmill Hill quartzite (Kinny 1990). These results reveal an age spectrum ranging from 3735 ± 10 Ma to 3177 ± 15 Ma, indicating derivation from a pre-existing granite-gneiss terrain similar in age to the Narryer Gneiss Complex (Kinny et al. 1990). Apart from these detrital zircons, no trace of an Early Archaean (>3.5 Ga) basement has been identified in the southwest areas of the JMB. Nieuwland and Compston (1981) reported conventional multi-grain zircon ages of ca. 3250 Ma for orthogneisses in the belt and a U-Pb age of ca. 3180 Ma for zircon cores from a migmatite, which they interpreted as dating the granulite facies metamorphism. These authors also reported combined zircon ages of 2670 ± 45 Ma for two post-tectonic granites.

Recent studies however, have brought some important modifications to this framework. The quartzite zircon results of Kinny (1990) have revised the maximum age of sedimentation of the Jimperding belt to 3177 Ma. In addition, Nemchin et al. (1994) determined ages of 2650–2640 Ma for zircons from mafic granulites from throughout the southwestern Yilgarn Craton, including an age of 2649 ± 6 Ma for zircons from two samples of granulites from Mount Dick at the eastern edge of the Jimperding belt. These authors interpreted these zircons as metamorphic and the age as dating the regional granulite facies metamorphism. Support for significant geological events at ca. 2650 Ma in the Toodyay area is provided by the results of a geochronological study of the Katrine syenite (Pidgeon et al. 1996), which occurs immediately adjacent to the granites and metasediments investigated in the present study (figure 2). Conventional U-Pb analyses on single zircons and SHRIMP analyses on euhedral zircons and zoned rims define a magmatic age of 2654 ± 6 Ma for the syenite, identical to the age of Nemchin et al. (1994) for the regional granulite facies metamorphism. In addition, SHRIMP analyses on zircon cores and unzoned zircon grains demonstrate that the zircon population contains a ca. 3250 Ma inherited component also detected on titanite. These results agree with those of Nieuwland and Compston (1981) in pointing out the significance of ca. 3250 Ma crustal rocks as a basement for the Jimperding belt. However, results to date have not confirmed the 3180 Ma granulite facies metamorphic event or the prolonged amphibolite facies metamorphism and migmatization at 2560–2500 Ma proposed by Nieuwland and Compston (1981).

Samples from the Katrine Area. Sample locations are shown on figure 2. Detailed sample descriptions (in an Appendix), are available from *The Journal of Geology* upon request. The orthogneiss (W400) is a medium-grained rock of granodioritic composition with a strong deformation fabric. This is in tectonic contact with the Katrine syenite on its western side and is flanked by a package of metasediments consisting of bands of sillimanite-quartz-muscovite schists, actinolite schists, and quartzites to the east. These units appear to have been strongly deformed and folded during events suspected as being coincident with the high-grade metamorphism. The sillimanite schists are vari-

able in their quartz content and range from pelitic (W398) to semi-pelitic (W399). One sample of pelitic schist (W402) was from a small outcrop of this rock type within the orthogneiss and may represent a large xenolith or a piece of schist folded into the orthogneiss. The amphibolite forms a lens adjacent to a large quartzite band. The porphyritic granite (W401) is variably deformed and is also concordant with the other units, although at one location it appears to intrude the schists. On present evidence, contact relationships are tectonic and do not provide a relative order of events. Our tentative interpretation of the geology is that original psammitic-quartzitic units, and units such as the amphibolite (W403), were intruded by granodiorite (the orthogneiss) and possibly the Katrine syenite, immediately preceding major deformation and metamorphism. In the schists (W398 and W399), the presence of sillimanite and cordierite and the absence of garnet indicate high temperature-low pressure metamorphic conditions. The occurrence of muscovite and the general absence of K-feldspar indicates that the rocks formed at metamorphic grades below the K-feldspar isograd where muscovite and quartz break down to K-feldspar and sillimanite. This reaction takes place at approximately 600°C at 2 kbar to 700°C at 5 kbar and we estimate the temperature for the amphibolite facies metamorphic overprint to be between 650° and 700°C.

Analytical Method

Mineral Selection. Zircons, monazites, titanites, and apatites were separated from 10–30 kg rocks by conventional mineral separation methods including Wilfley Table, high-density liquids, and a Frantz magnetic separator. The selection of minerals, based on the morphology, homogeneity, and transparency is of critical importance for this type of geochronological study. Only the best-quality grains (inclusion-free, no fractures or cores) were selected. In order to remove discordant domains, air abrasion (Krogh 1982) was applied to all zircon crystals analyzed conventionally. Monazites from the three metasediments (W398, W399, and W402) have rounded shapes, typical of grains formed under metamorphic conditions (e.g., Parrish 1990), and the grains chosen for analyses were as colourless (pale yellow) and free of inclusions as possible.

Analytical Procedures. Zircons, titanites, and monazites were weighed with an electronic microbalance and placed in a Teflon dissolution capsule (Parrish 1987) with a drop of tridistilled 48% HF (6N HCl for monazite) and spiked with a ^{205}Pb-^{235}U tracer. The capsule was mounted into a steel bomb, and the assemblage was held for 3 to 4 days at 195°C. After dissolution, the solution was evaporated to dryness and then redissolved with tridistilled 6N HCl in the steel bomb overnight. Apatites were dissolved in a Savillex teflon beaker on a hot plate with 6N HCl. Lead and uranium were separated on microcolumns following the chemistry previously described by Krogh (1973). For titanite, monazite, and apatite, an additional purification step for the uranium was performed following the procedure described by Manhes et al. (1978). Isotopic measurements were carried out on a VG 354 mass spectrometer using a Daly detector for small sample loads. Pb and U were loaded with silica gel and phosphoric acid on a single filament. Pb was analysed at 1400°–1450°C and U at 1500°–1550°C. A mass discrimination correction for measurements on the Daly of 0.28 ± 0.05% per amu was determined from the NBS common lead (NBS981) and uranium (U500) standards. Total Pb blanks over the period of the analyses range from 8 to 20 pg, and uranium blanks were <5 pg. The isotopic composition of radiogenic Pb was determined by subtracting first the blank Pb and then the remainder, assuming a common Pb composition at the time of initial crystallization as determined from the model of Stacey and Kramers (1975). Calculations were made using the program of Ludwig (1987). Analytical uncertainties are listed as 2σ, and uncertainties in ages as 95% confidence levels. Decay constants are those determined by Jaffey et al. (1971) and recommended by the IUGS Subcommission on Geochronology (Steiger and Jäger 1977). For SHRIMP analyses, zircon grains were mounted in epoxy resin and polished to approximately half their thickness to reveal interior structures. Mounts were then cleaned and gold-coated, and U-Th-Pb analyses were performed using the SHRIMP II ion microprobe at the Curtin University of Technology (Perth), following the techniques of Compston et al. (1984) and Williams et al. (1984). Pb/U ratios were normalized via quadratic working curves to those measured on the standard CZ3 ($^{206}Pb/^{238}U = 0.0914$) prepared from a gem quality Sri Lankan zircon (Pidgeon et al. 1994). Results have been reported on concordia plots and are represented according to their 1σ and 2σ error boxes for SHRIMP and conventional analyses, respectively.

Results

The petrographic description of each sample (figure 2) is presented in the Appendix available from *The*

Sample		Weight	U	Pb	$^{206}Pb/^{204}Pb$	$^{207}Pb/^{206}Pb$	$^{208}Pb/^{206}Pb$	$^{206}Pb/^{238}U$	$^{207}Pb/^{235}U$	$^{207}Pb/^{206}Pb$	7/6 age (Ma)	Disc. (%)
		(mg)	(ppm)	(ppm)	Measured Ratios			(±2σ)	(±2σ)	(±2σ)	(±2σ)	
Orthogneiss W400	01.Zr. lp	.011	139	83	1062	.1891	.201	.5120±22	12.79±06	.1812±05	2664±4	0.0
	02.Zr. lp	.007	97	55	1073	.1866	.162	.5003±37	12.48±10	.1810±04	2662±4	1.8
	03.Zr. lp	.003	313	176	1944	.1857	.111	.5138±29	12.86±07	.1815±03	2667±3	-0.2
	04.Zr. lp	.002	236	142	1267	.1883	.208	.5122±41	12.82±11	.1815±05	2667±4	0.0
	05.Zr. lp	.008	74	48	689	.1928	.342	.5062±41	12.71±11	.1821±05	2672±5	1.2
	06.Zr. lp	.002	186	110	930	.1914	.203	.5096±57	12.77±15	.1817±06	2668±5	0.5
	07.Ti. yl	.033	206	129	943	.1911	.294	.5048±10	12.51±04	.1798±05	2651±4	0.6
	08.Ti. yl	.032	231	139	1676	.1856	.213	.5048±10	12.51±03	.1798±03	2651±2	0.6
	09.Ti. yl	.084	173	111	568	.1991	.353	.5007±10	12.35±07	.1789±08	2643±7	1.0
	10.Ti. yl	.014	195	125	1156	.1886	.323	.5032±13	12.45±04	.1795±03	2648±3	0.8
	11.Ti. yl	.028	112	71	928	.1901	.363	.4822±13	11.96±05	.1799±04	2652±4	4.3
	12.Ti. yl	.034	86	57	777	.1923	.371	.5035±13	12.46±05	.1795±05	2649±5	0.8
	13.Ap. mlt	.024	31	27	143	.2611	.537	.5080±54	12.58±27	.1796±30	2649±27	0.0
	14.Ap. mlt	.032	25	21	147	.2577	.544	.4926±55	12.14±26	.1787±28	2641±26	2.2
	15.Ap. mlt	.058	20	14	127	.2678	.570	.3994±52	9.85±25	.1789±34	2642±32	18.0
Granite W401	16.Zr. lp	.004	238	115	1258	.1882	.180	.4197±27	10.51±07	.1816±04	2667±3	15.0
	17.Zr. lp	.007	114	61	1114	.1875	.203	.4542±31	11.38±08	.1817±04	2669±3	9.5
	18.Zr. lp	.013	192	109	2513	.1850	.154	.4884±11	12.23±03	.1816±02	2668±2	3.9
	19.Zr. lp	.018	290	131	1173	.1903	.207	.3717±10	9.29±03	.1813±03	2664±3	23.5
	20.Zr. lp	.019	290	131	846	.1943	.215	.3673±13	9.18±04	.1812±05	2664±4	24.3
	21.Mo. yl	.003	1375	4167	499	.2013	5.687	.4847±14	12.08±07	.1808±08	2660±7	4.2
Amphibolite W403	22.Zr. lp	.006	998	553	3908	.1820	.102	.5012±11	12.43±03	.1799±01	2652±1	1.3
	23.Zr. lp	.007	1146	627	10989	.1811	.071	.5083±10	12.68±03	.1809±01	2661±1	0.4
	24.Zr. lp	.004	694	384	2540	.1840	.103	.5044±19	12.55±05	.1804±02	2657±2	0.9
	25.Zr. lp	.005	1096	603	7943	.1808	.088	.5048±10	12.55±03	.1803±01	2656±1	0.8
	26.Zr. lp	.006	876	473	7429	.1815	.053	.5097±11	12.71±03	.1808±01	2661±1	0.2
	27.Zr. lp	.002	619	347	3142	.1833	.110	.5073±18	12.64±05	.1807±02	2659±2	0.5
	28.Zr. lp	.003	1166	642	2157	.1851	.131	.4850±14	12.06±04	.1804±02	2656±2	4.0
	29.Ti. or	.008	63	55	399	.2114	.713	.5198±23	13.36±09	.1864±08	2711±7	0.4
	30.Ti. dk	.013	116	67	422	.2098	.758	.3146±09	8.00±05	.1843±08	2692±8	35.0
	31.Ti. dk	.012	56	65	235	.2352	.798	.4680±19	12.04±14	.1865±17	2712±15	8.8
Schist W398	32.Mo. yl	.009	4203	8161	13004	.1800	3.194	.5079±09	12.65±02	.1806±01	2659±1	0.4
	33.Mo. yl	.006	4826	9368	6557	.1818	3.173	.5100±09	12.74±02	.1812±01	2664±1	0.3
	34.Mo. yl	.005	5471	9731	6105	.1817	2.835	.5070±09	12.65±02	.1810±01	2662±1	0.7
	35.Mo. yl	.008	2730	6332	8569	.1800	4.035	.5072±09	12.58±02	.1799±01	2652±1	0.3
	36.Mo. yl	.006	4824	9360	5160	.1821	3.170	.5099±09	12.75±03	.1813±01	2665±1	0.3
Schist W399	37.Mo. yl	.004	2828	6384	1772	.1856	3.832	.5104±10	12.71±03	.1807±02	2659±2	0.0
	38.Mo. yl	.007	1917	5811	1325	.1872	5.645	.4992±09	12.44±03	.1808±03	2660±3	1.9
	39.Mo. yl	.009	2303	7486	2537	.1829	6.052	.5088±09	12.69±03	.1808±02	2661±2	0.3
	40.Mo. yl	.003	4687	10219	3470	.1829	3.644	.5158±10	12.86±03	.1809±02	2661±2	-0.8
	41.Mo. yl	.005	1688	6848	1820	.1840	7.884	.5027±10	12.54±03	.1809±02	2661±2	1.3
Schist W402	42.Mo. yl	.025	3596	6576	31646	.1809	2.987	.5047±16	12.60±04	.1811±01	2663±1	1.1
	43.Mo. yl	.005	6855	10788	17668	.1805	2.428	.5005±09	12.50±02	.1811±01	2663±1	1.7
	44.Mo. yl	.008	5549	13552	5450	.1811	4.459	.4952±09	12.30±03	.1801±02	2654±2	2.3
	45.Mo. yl	.005	4604	10483	11274	.1801	4.031	.4996±08	12.45±02	.1807±01	2659±1	1.8
	46.Mo. yl	.006	4316	8447	5163	.1810	3.355	.4951±20	12.23±05	.1792±02	2645±2	2.0

Table 1. Conventional U-Pb data for accessory minerals from rocks from the Toodyay area of the Jimperding Metamorphic Belt (Western Australia). Uncertainties are given at the two-sigma level. Zr. zircon; Ti; titanite; Mo: monazite; Ap: apatite; mlt: multiple grain analysis; lp: light pink, yl: yellow translucent; or: orange; dk: dark brown.

Journal of Geology. U-Pb Results are reported on table 1 and table 2.

Orthogneiss W400. Conventional analyses of six abraded single zircon grains yielded essentially concordant and overlapping data points (figure 3*a*) that define a regression line (MSWD = 2.9) with intercept ages of 2667 ± 6 and 297 ± 908 Ma. The wide uncertainty of the lower intercept age allows for the possibility that this is not significantly different from zero and may be related to uplift and exposure. Of the six grains analyzed, four (grains 1, 3, 4, and 6) plot within 1% of the concordia curve and provide a $^{207}Pb/^{206}Pb$ weighted mean age of 2666 ± 2 Ma (MSWD = 0.8).

Fourteen zircon grains have been analyzed for U-Th-Pb isotopes using the SHRIMP II ion microprobe (figure 3*b*, table 2). Individual $^{207}Pb/^{206}Pb$ ages range from 2684 ± 14 Ma (2σ) to 2636 ± 16

Sample	Grain spot	U (ppm)	Th (ppm)	Th/U	*Pb (ppm)	^{204}Pb (ppb)	^{206}Pb/^{204}Pb	^{208}Pb/^{206}Pb	^{206}Pb/^{238}U (±1σ error)	^{207}Pb/^{235}U (±1σ error)	^{207}Pb/^{206}Pb (±1σ error)	7/6 age ±1σ (Ma)	Disc. (%)
W398	1-1	360	609	1.69	332	227	2493	.465	.629±11	22.51±44	.2595±18	3244±11	3
	2-1	758	273	.36	548	323	4605	.113	.644±11	18.69±33	.2105±06	2910±05	-10
	3-1	264	71	.27	180	55	3124	.074	.606±11	19.71±37	.2359±10	3093±07	1
	4-1	242	93	.38	173	83	1407	.098	.617±11	21.13±40	.2486±12	3176±08	2
	5-1	827	845	1.02	640	171	4280	.273	.600±10	19.05±34	.2305±08	3055±06	1
	6-1	355	220	.62	302	44	1599	.149	.683±12	26.76±49	.2841±11	3386±06	1
	7-1	513	295	.57	439	100	3040	.147	.690±12	27.93±50	.2935±09	3436±05	2
	8-1	277	104	.38	206	46	3291	.109	.636±11	21.57±40	.2460±11	3159±07	0
	9-1	226	80	.35	204	49	2935	.089	.746±13	32.34±61	.3145±14	3543±07	-1
	10-1	230	178	.77	218	107	935	.192	.728±13	30.67±58	.3055±15	3498±08	-1
	11-1	162	140	.86	115	183	548	.212	.555±10	19.27±41	.2517±22	3196±14	11
	12-1	682	287	.42	391	328	1491	.126	.495±08	16.06±29	.2354±08	3089±06	16
W400	1-1	317	163	.51	179	562	239	.141	.495±10	12.37±27	.1813±06	2665±06	3
	1-2	357	101	.28	196	151	1027	.078	.507±11	12.65±27	.1809±05	2661±05	1
	2-1	321	81	.25	176	190	736	.069	.509±11	12.78±26	.1819±05	2670±05	1
	2-2	553	170	.31	287	335	672	.085	.476±10	11.91±25	.1814±04	2666±04	6
	3-1	360	201	.56	206	5	29521	.151	.499±10	12.50±27	.1817±05	2668±04	2
	3-2	212	122	.57	123	8	11027	.156	.504±11	12.52±28	.1802±07	2655±07	1
	4-1	404	70	.17	221	2	80756	.048	.519±11	12.91±28	.1804±05	2657±05	-1
	5-1	151	108	.71	88	2	28850	.194	.490±10	12.39±27	.1834±08	2684±07	4
	5-2	154	140	.91	95	2	27018	.242	.501±11	12.50±29	.1809±08	2662±07	2
	5-3	109	79	.72	65	1	35984	.196	.499±11	12.36±28	.1798±10	2651±09	2
	5-4	139	119	.86	87	8	7230	.240	.516±11	12.73±28	.1788±08	2642±07	-2
	6-1	426	105	.25	231	7	25002	.065	.507±11	12.65±27	.1809±04	2661±04	1
	6-2	339	104	.31	179	17	8208	.082	.484±10	12.16±26	.1820±06	2672±05	5
	7-1	124	78	.63	73	5	11916	.165	.509±11	12.50±28	.1782±09	2636±08	-1
	8-1	187	149	.80	115	45	1828	.227	.508±11	12.63±29	.1803±12	2656±11	0
	9-1	416	134	.32	232	6	30317	.087	.510±11	12.72±27	.1807±04	2659±04	0
	10-1	204	117	.57	121	3	30125	.154	.516±11	12.89±28	.1814±06	2665±06	-1
	10-2	289	153	.53	157	10	11494	.134	.480±10	11.95±26	.1804±06	2657±05	5
	11-1	580	271	.47	332	10	22279	.127	.508±11	12.65±27	.1807±04	2659±03	0
	11-2	260	95	.37	159	3	43560	.097	.557±11	13.85±30	.1803±05	2656±05	-7
	12-1	69	73	1.07	44	5	5883	.293	.504±11	12.55±30	.1806±15	2658±13	1
	12-2	45	28	.64	26	3	6748	.169	.509±11	12.71±32	.1811±17	2663±16	0
	13-1	251	151	.60	150	3	40657	.163	.516±11	12.92±28	.1816±06	2668±05	-1
	13-2	181	93	.51	104	1	98736	.141	.507±11	12.65±28	.1809±07	2662±06	1
	14-1	129	86	.70	73	18	2949	.181	.510±11	12.56±29	.1787±12	2641±11	-1

Table 2. Ion-microprobe U-Th-Pb data for zircons analysed from the metasediment W398 and from the orthogneiss W400 (Jimperding Metamorphic Belt). First number: grain, second number: spot.

Ma (2σ). The maximum value is from a core of unzoned (unetched by HF) zircon (#5-1) and is interpreted as an inherited xenocryst overgrown by magmatic zircon (as demonstrated by analyses #5-2 and #5-3: see table 1) or, owing to the slight difference in age, an earlier phase of the same episode of magmatic crystallization. A tight close to concordant group of data points (21 analyses on 12 grains) on zoned zircon provides a ^{207}Pb/^{206}Pb weighted mean age of 2662 ± 4 Ma, in good agreement with the age obtained by conventional method (2666 ± 2 Ma). SHRIMP spots on patches of unzoned zircon (#5-4, 7-1, and 14-1), which appear to transgress the zoning, give a younger ^{207}Pb/^{206}Pb weighted mean age of 2640 ± 16 Ma. Reported on a ^{208}Pb/^{206} Pb versus Th/U diagram (figure 3*c*), all data plot on a single line and show very little deviation from closed-system behavior in ancient times. Unzoned patches have a similar range of U, Th, and Th/U to that observed for analyses on zoned domains. These data are tentatively interpreted as having been disturbed during the high-grade metamorphic episode dated at ca. 2650 Ma (Nemchin et al. 1994).

Conventional analyses were made on six single grains of euhedral titanites. All analyses but one (analysis 11) plot within 1% of the concordia curve (figure 3*d*) and have identical ^{207}Pb/^{206}Pb ages (table 1) ranging from 2643 ± 7 Ma to 2652 ± 4 Ma. On the concordia diagram they define a chord (MSWD = 2.05) that intersects with the Concordia at 2649 ± 4 and −110 ± 500 Ma.

Three analyses were performed on a multigrain fraction of apatite. Analysis 13 is concordant at 2649 ± 27 Ma, whereas analyses 14 and 15 are 2 and 18% discordant, respectively. On the Concordia diagram (figure 3*e*), they define an alignment (MSWD = 0.3) providing an upper intercept of 2644 ± 19 Ma and a near-zero lower intercept (−197 ± 340 Ma). The relatively high uncertainties in the apatite ages are the result of the low uranium content of this mineral and consequently

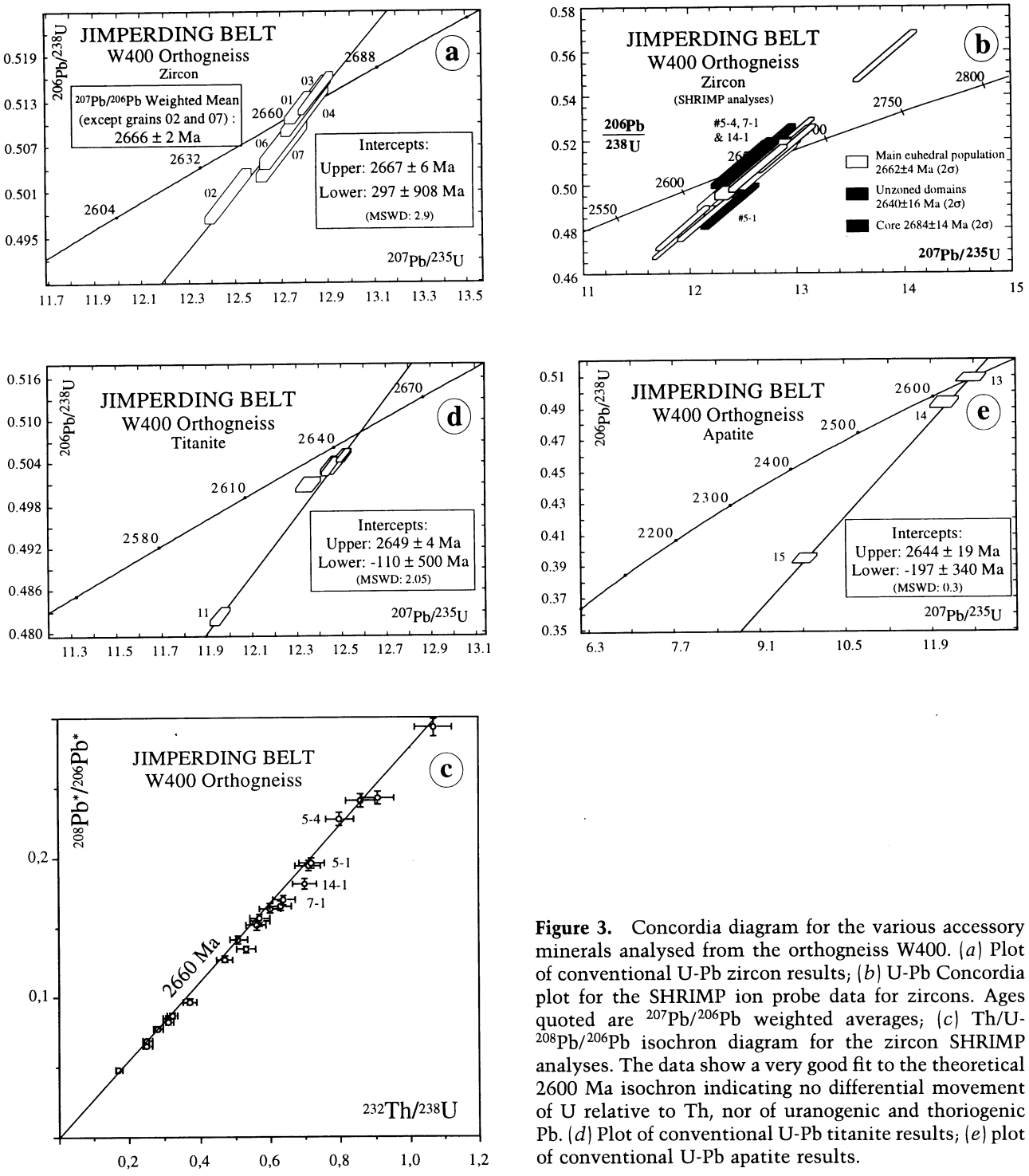

Figure 3. Concordia diagram for the various accessory minerals analysed from the orthogneiss W400. (*a*) Plot of conventional U-Pb zircon results; (*b*) U-Pb Concordia plot for the SHRIMP ion probe data for zircons. Ages quoted are $^{207}Pb/^{206}Pb$ weighted averages; (*c*) Th/U-$^{208}Pb/^{206}Pb$ isochron diagram for the zircon SHRIMP analyses. The data show a very good fit to the theoretical 2600 Ma isochron indicating no differential movement of U relative to Th, nor of uranogenic and thoriogenic Pb. (*d*) Plot of conventional U-Pb titanite results; (*e*) plot of conventional U-Pb apatite results.

of the relatively low ratio of radiogenic to common Pb.

Porphyritic granite W401. Zircon grains from this sample are euhedral to subhedral and range in color from light pink to translucent. Zoned and unzoned crystals are present and they generally contain randomly oriented rod- and needle-shaped inclusions. In spite of the low U content (114–290 ppm) (table 1) and strong abrasion, experimental points present a high degree of discordance, ranging from 3.9 to 24.3%. This is probably related to the occurrence of cracks in almost all grains,

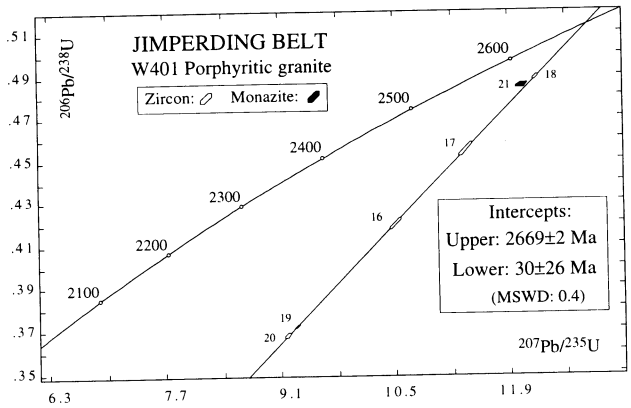

Figure 4. Concordia plot showing conventional results on zircon and monazite from the porphyritic granite (W401).

which is likely to facilitate U-Pb disturbance. Reported on the concordia diagram (figure 4), the five single grains fit a perfect line (MSWD = 0.4) yielding ages of 2669 ± 2 and 30 ± 26 Ma for the upper and lower intercepts, respectively. Zircon morphology suggests an igneous origin, and there is no suggestion from the isotopic results that the zircon population contains older inherited grains. Therefore, the upper intersection (2669 ± 2 Ma) is interpreted as the age of zircon crystallization and emplacement of the porphyritic granite. The alignment of the data points and the close-to-zero lower intercept age (30 ± 26 Ma) can be explained as recent lead loss probably during uplift and erosion or as a result of surficial alteration (Stern et al. 1966; Goldich and Mudrey 1972; Black 1987). This also indicates that the zircons have not undergone isotopic disturbances in Archean or Proterozoic times.

The analysis of one single crystal of monazite gave a discordant data point (table 1, figure 4) with a $^{207}Pb/^{206}Pb$ age of 2660 ± 7 Ma. Although this age is in the range of the $^{207}Pb/^{206}Pb$ ages for zircon grains (from 2664 to 2669 Ma), the data point plots slightly to the left of the zircon line, raising the possibility that the younger monazite age is real and represents a cooling age or a slightly younger disturbance of the U-Pb systems.

Amphibolite W403. The sample, taken from an amphibolite band flanking a thick quartzite unit, is locally invaded by a network of millimeter to centimeter thick leucocratic veinlets. It was not possible to separate pure amphibolite from amphibolite plus leucocratic veinlets so, after crushing to approximately 3 cm cubes, the sample was divided into two parts: a sample with lots of veinlets and a second sample with a minimum of veinlets. Zircons and titanites were recovered from both samples. The yield of zircons from the leucocratic vein-dominated sample greatly exceeded that from the sample with fewer veins, indicating that zircons are concentrated in the veins. This is consistent with the fact that zircons in both samples are of similar morphology. Conventional analyses of single zircons have high U concentrations (betwen 619 and 1166 ppm) indicating crystallization from a U-rich phase and precluding an origin from the amphibolite itself. The grains present euhedral shapes attributed to an igneous origin, and no inherited component has been recognized in this zircon population. Three analyses (23, 26, and 27) are within 0.5% of the concordia and provide an average $^{207}Pb/^{206}Pb$ age of 2661 ± 1 Ma (figure 5). The other four grains (22, 24, 25, and 28) are slightly discordant and have younger ages ranging from 2652 ± 1 to 2657 ± 2 Ma, suggesting that they have undergone early (Archean) Pb loss. Regressing all seven data points would not significantly change the upper intercept (2661 ± 3 Ma) but would increase the lower intercept age to 387 ± 560 Ma, which is not significantly different from zero and the result of a long extrapolation. We conclude that the concordant or nearly concordant grains, which had their surfaces removed by air abrasion, date crystallization of zircons within the leucocratic veins.

Three crystals of titanite, separated from the melanocratic part of the amphibolite, have been analyzed (table 1). Analysis 29 is nearly concordant at 2711 ± 7 Ma and, on the Concordia diagram (figure 5), the three points define an alignment (MSWD = 0.3) with an upper intercept of 2711 ± 7 Ma and a close to zero lower intercept (76 ± 39 Ma). The 2711 Ma age is significantly older than the age of zircons in the leucocratic veins. It may represent the age of emplacement of the original mafic rock in the surrounding sediments or it may date an earlier metamorphic event that resulted in the growth of titanite. The preservation of chronological information by titanites also implies that temperature conditions, since ca 2.7 Ga and especially during formation of the veins, did not exceed the thermal blocking temperature of titanite, estimated to be 650 ± 20°C for grains with effective diffusion radii of 100–500 μm (Cherniak 1993), in the size range of the titanite from the amphibolite.

Psammopelite W399. Abundant, rather large monazite crystals (75–135 μm) were found in this schist sample. The monazite grains are clear, pale yellow, and typically have rounded shapes characteristic of growth under metamorphic conditions (Parrish 1990). Zircons were recovered from this

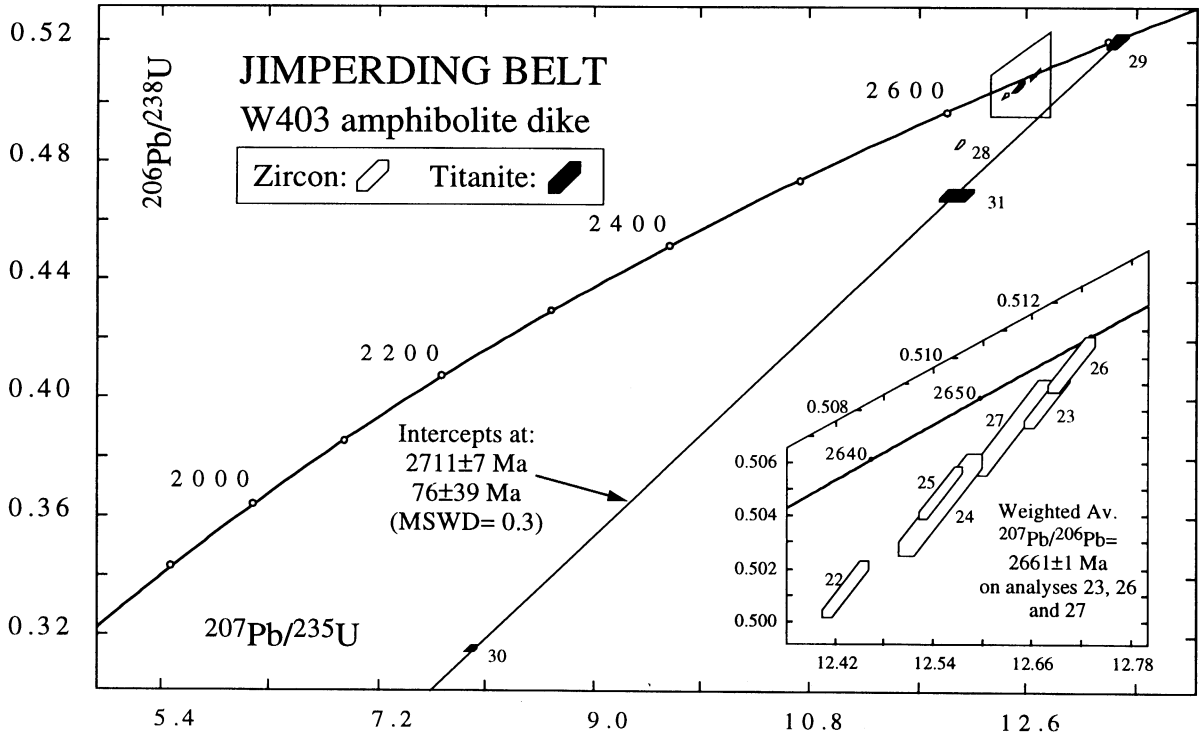

Figure 5. Concordia diagram showing conventional analyses for zircons and titanites extracted from the amphibolite W403.

sample but were too small (<74 μm) for single zircon dating, and multigrain analyses have not been performed. All five monazite analyses plot within 2% of the concordia (figure 6, table 1), and they provide upper and lower intercepts of 2661 ± 1 and 18 ± 206 Ma (MSWD = 0.9). Analysis 40 is slightly above discordia (0.8%) but still has a $^{207}Pb/^{206}Pb$ age of 2661 Ma, suggesting that this might be due to incomplete dissolution (although no residue was apparent in the bomb capsule). In this area of the Jimperding Belt, the metamorphic grade is middle to upper amphibolite facies, slightly below the closure temperature of monazite (725 ± 25°C as estimated by Copeland et al. 1988). The 2661 ± 1 Ma age therefore dates new growth and crystallization of monazite in the pelitic/psammitic schist during the increase of heat accompanying the amphibolite facies metamorphism.

Pelitic Schist W398. Zircons and monazites were recovered from this sample. The results of SHRIMP II analyses (table 2) of rounded zircon grains are shown on figure 7. Most analyses are within 5% of the concordia and U-Pb ages range from concordant to up to 16% discordant. The age spectrum clearly indicates a heterogeneous provenance for the detrital zircons analysed. They exhibit $^{207}Pb/^{206}Pb$ ages in the range 3055 to 3543 Ma. Grain #2 with one of the highest U contents (758 ppm), has a younger apparent age of ca. 2910 Ma, but plots above discordia, suggesting abnormal behavior or unknown analytical error. It has not been taken into account in this discussion. The old zircons indicate the presence of early Archean crust in the provenance, in agreement with the results of

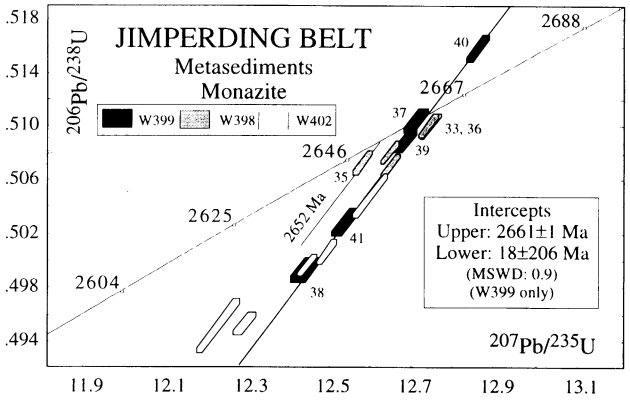

Figure 6. Concordia diagram showing conventional analyses of single monazite grains from schists samples W398, W399 and W402. The regression line and intercepts have been calculated for single monazite grains from W399.

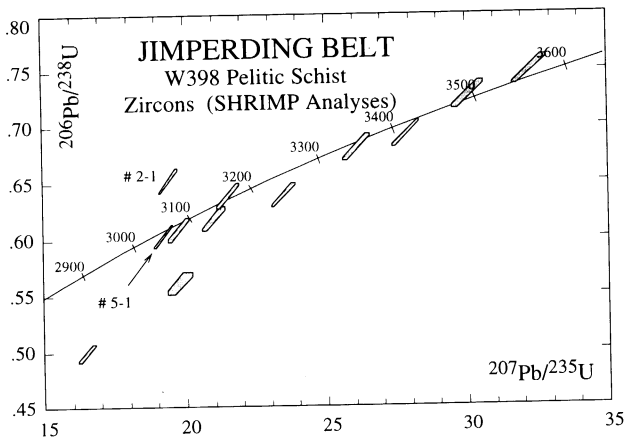

Figure 7. Concordia plot showing SHRIMP U-Pb results on detrital zircon grains from the pelitic schist W398.

Kinny (1990) on the Windmill Hill quartzite. The youngest concordant age of 3055 ± 12 Ma (2σ) from analysis #5-1 provides a maximum age for the deposition of the pelitic sediments. This age is younger than the estimate of 3177 ± 15 Ma (2σ) based on zircons from the Windmill Hill quartzite in the Toodyay area (Kinny 1990) but is broadly similar to the ca. 3100 Ma upper limit for deposition of the mount Narryer and Jack Hills metasediments from the northern part of the Western Gneiss Terrain (Compston and Pidgeon 1986; Kinny et al. 1990).

Monazites separated from this sample have similar rounded forms to those of sample W399. Five single crystals were analyzed conventionally and provide concordant to sub-concordant points, plotting within 1% of the concordia (figure 6, table 1). Results, however, are less straightforward than for sample W399, as monazite analyses show a lateral dispersion on the concordia plot expressed by $^{207}Pb/^{206}Pb$ ages spanning 13 Ma from 2652 to 2665 Ma. These observations suggest that monazite growth has been influenced by more than one event. (The question of why the monazites in the same rock have different ages is addressed in the discussion.)

Pelitic Schist W402 (Xenolith in Porphyritic Granite W401). Monazite analyses were made on five rounded, pale yellow single grains. As for the previous sample W398, the monazite data points do not define a single line on a concordia plot (figure 6). The inhomogeneity of the data is also reflected in the $^{207}Pb/^{206}Pb$ ages, which range from 2645 ± 2 to 2663 ± 1 Ma (table 1), and the degree of discordance, which is relatively greater than for monazite analyses in the other samples. The three least discordant analyses (42, 43, and 45) have $^{207}Pb/^{206}Pb$ ages that overlap the 2661 Ma age of monazite from sample W399. The two other analyses have younger $^{207}Pb/^{206}Pb$ ages and higher discordance.

Discussion

Early History. SHRIMP U-Th-Pb analyses of detrital zircons from the pelitic schist (W398) indicate that the clastic sediments of the JMB contain zircon grains with ages ranging from 3055 to 3550 Ma (figure 7). The age spectrum does not show any definite age groupings but is consistent with previously published results (Kinny 1990) confirming the original sedimentary material was contributed from an older Archean source. The youngest concordant grain (#5-1) from the detrital zircon suite from sample W398 indicates a maximum age for deposition of sediments in the JMB of 3055 ± 12 Ma. Titanites from an amphibolite (W403), suspected of being an early dike in the metasediments, give an age of 2711 ± 7 Ma (figure 5). This may be the age of emplacement of the original diabase, or it may date the formation of titanite by metamorphic reaction during an early stage in the episode of igneous emplacement and high-grade metamorphism. In either case, the titanite age provides a minimum age for sedimentation. These two limits constrain deposition of sediments of the JMB at between 2711 and 3055 Ma. This period is identical to the 2750–3050 Ma interval proposed by Nutman et al. (1991) for deposition of the Jack Hills/Narryer supracrustal association in the northwest Yilgarn Craton. The two series contain BIF (Wilde 1980) and shallow water sediments, suggesting that the sediments formed by shallow water sedimentation alongside an Early Archean crustal segment. The oldest ages indicate an Early Archean (ca. 3550 Ma) component in the source. However, no zircons ages as old as ca. 3.7 Ga appeared, such as found in zircons from gneisses from the Narryer and Jack Hills region in the northwest Yilgarn, suggesting that the source rocks were not identical. It is also puzzling that there is no distinct grouping of ages corresponding with the 3250 Ma age of zircons and titanites from the Katrine syenite (Pidgeon et al. 1996) and zircons from the orthogneisses (Nieuwland and Compston 1981). These ages in the syenite suggest that 3250 Ma granitic rocks could have formed the platform for the accumulation of the Jimperding Belt at 3055–2711 Ma. However, the lack of such zircons in samples of metasediment indicate that the sediments were derived from source rocks independent of the 3250

Ma old crust identified in the gneisses and the syenite.

Timing of Plutonism, Metamorphism and Cooling. A comparison of zircon results on samples of orthogneiss (W400) and deformed porphyritic granite (W401) provides evidence for the age of crystallization of the granites. Conventional regression ages of zircons from these samples are indistinguishable at the 2σ level (2667 ± 6 and 2669 ± 2 Ma respectively), and we conclude on this evidence that crystallization of granitic magma occurred in the period 2660–2670 Ma. SHRIMP analyses of zircons from the orthogneiss (W400) were focused on structural parts of the zircons to test the uniformity of the U-Pb ages within the zircons and to examine any correlations of ages with structural elements. No very old zircon xenocrysts or cores were clearly identified, although the core of one grain #5-1) had an age of 2684 ± 14 Ma. SHRIMP analyses of areas of zircons (W400) that consisted of multiple, fine, euhedrally zoned zircon gave a consistent $^{207}Pb/^{206}Pb$ weighted mean age of 2662 ± 4 Ma (figure 3*b*). Although identical within uncertainty to the conventional age, this is a minimum of about 5 m.y. younger. This age bias might be explained by considering that the conventional results on abraded grains contain slight amounts of core material not detected during optical examination. In view of this we accept the younger SHRIMP age of 2662 ± 4 Ma as the best estimate for the emplacement of the granodiorite. This is in line with the age of zircons extracted from the leucocratic veins infiltrating the amphibolite band W403, which falls in this interval (2661 ± 1 Ma) (inset in figure 5). These micro-veinlets probably formed by fine-scale injection of granitic magma into the amphibolite precursor during metamorphism and brittle fracturing accompanying emplacement of the crystallizing granitoids. SHRIMP ages were also determined on outer unzoned rims and domains. These were generally younger with an average of $^{207}Pb/^{206}Pb$ weighted mean age of 2640 ± 16 Ma, similar to the age of regional metamorphism dated at ca 2650 Ma by Nemchin et al. (1994) (figure 3*b*). The granitoids (W400, W401) have been deformed and metamorphosed to amphibolite facies during this regional metamorphism, and we propose that this event is responsible for the younger ages determined for unzoned rims. However, this event has not affected ages determined by conventional analyses of abraded grains or SHRIMP analyses of zoned zircon. The period of granitoid emplacement (2660–2670 Ma) determined in this study is in good agreement with the 2670 ± 45 Ma age attributed to granitoid crystallization in the Toodyay district by Nieuwland and Compston (1981).

Monazite, is, after zircon, probably the most used U-rich phase in geochronology. This mineral is often thought to have a relatively simple U-Pb system in comparison with zircon. Recent studies, however, have highlighted complexities in the behavior of this mineral such as inheritance (Copeland et al. 1988), recrystallization (DeWolff et al. 1993), and Pb loss during a metamorphic event (Black et al. 1984). Nevertheless, monazite represents a powerful geochronometer, especially in the dating of metamorphic events. In metamorphic terranes this mineral forms by the destabilization of precursors such as apatite and allanite or Th- and REE-rich oxides, when sediments are subjected to lower amphibolite facies conditions (Kingsbury et al. 1993). Smith and Barreiro (1990) have shown that, in pelitic sediments, monazite growth occurs at the staurolite isograd, at a temperature of about 525 ± 25°C, and that once formed, monazite remains closed to isotopic exchange even if subjected to a higher temperature. In the Toodyay area, amphibolite facies metamorphism with P-T conditions in the range of 650°–700°C and 2 to 5 kbar is favourable for monazite growth, and this mineral is found in pelitic and psammitic schists. Monazites analyzed are round to tabular grains typical of metamorphic monazites (Parrish 1990). Conventional U-Pb isotopic analyses of monazites from the sample of psammitic schist (W399) provide a precise age of 2661 ± 1 Ma (table 1, figure 6), within uncertainty of the age of zircon crystallization in the deformed granodiorite and identical to the age of 2660 ± 7 Ma for a monazite grain from the porphyritic granite (table 1). However, the consistent picture presented by the ages of monazites from these samples is not suported by the results of monazites from two other samples of pelitic schist (W398 and W402), which show a significant spread in $^{207}Pb/^{206}Pb$ ages from 2665 ± 1 Ma to 2645 ± 1 Ma. This age spread can be interpreted as indicating that more than one geneation of monazite is present, or that the monazites in these two schists have responded inhomogeneously to a common metamorphic history. The two oldest grains from sample W398 (analyses 33 and 36) (table 1, figure 6) have ages (2664 ± 1 and 2665 ± 1 Ma) between the ages of emplacement of the two granitoids. This suggests that monazite growth may have first occurred as a result of heating of the pelitic sediment during emplacement of the porphyritic granite. A number of data points are discordant on the concordia plot (figure 6); however, it appears that most grains plot close to the regression line calcu-

lated for grains from sample W399. This is consistent with the main monazite generation being ca. 2661 Ma. One grain (analysis 35) has a nearly concordant younger age of 2652 ± 1 Ma, which is the same, within errors, as the age of regional metamorphism of ca. 2650 Ma (Nemchin et al. 1994) and the age of zircon crystallization and major disturbance of the titanites recorded in the nearby Katrine Syenite (Pidgeon et al. 1996). In view of the predominance of ca. 2661 Ma monazites in the metasediments, we favor the interpretation that the main monazite generation formed by prograde metamorphic reaction at about 525°C at 2661 Ma and that the younger U-Pb ages reflect partial to complete Pb loss from some grains at about 2650 Ma, which corresponds to the peak of high-grade metamorphism. On the other hand, the preservation of grains older than the ca. 2661 Ma main generation (analyses 33 and 36), is interpreted as reflecting inhomogeneity within grains. This may be related to monazite inclusions that have first grown during emplacement of the porphyritic granite W401 at ca 2669 Ma and used as nuclei around which 2661 Ma old monazites may have grown when sediments passed through the ca. 500°C isograd.

Inhomogeneity in monazite ages within a single grain has been previously recorded by De Wolf et al. (1993) from ion microprobe measurements, and it is possible that the oldest monazites also have inhomogeneous age distributions within individual grains. In addition, recent studies (Copeland et al. 1988; Parrish and Turrul 1989; Smith and Barreiro 1990; De Wolf et al. 1993) have found that monazite is not reset by exposure to high temperatures for geologically significant periods of time and that the effective closure temperature for monazite is ≥700°C. The preservation of the first monazite generation may therefore not be surprising, taking into account the fact that growth occurred below the closure temperature of these minerals. Because of the closeness in age of the different domains (2669 and 2661 Ma), whole-grain analyses of these inhomogeneous grains produce only slightly discordant analytical points located between these two values. In summary, monazites in the schists appear to have formed during at least two growth episodes. A first generation probably accompanied the initial stages of granite emplacement at ca. 2669 Ma, while the main generation formed at 2661 Ma by prograde metamorphic reaction when sediments passed through the 500°C isograd. Some grains have undergone partial to complete updating at the peak of regional metamorphism at ca. 2650 Ma. The loss of radiogenic Pb from some grains as the temperature increased to a peak, close to 700°C, at ca. 2650 Ma, requires that the monazites in the schists to have responded nonuniformly to a common thermal history. However, the results may also be explained by proposing that some monazite grains were armored against Pb loss by incorporation in other grains.

Titanites from the orthogneiss W400 yield an age (2649 ± 4 Ma) younger than the zircon age of this rock (ca. 2662 Ma) (figure 3*d* and 3*b*), but similar, within-error margins to the SHRIMP age for patches of unzoned zircon, and to the age of the regional high-grade metamorphism. Titanite may have formed either by metamorphic reaction at a temperature of approximately 650°–700°C reached at the peak of metamorphism at 2650 Ma, or earlier but became a closed system at 2650 Ma. The titanite age is also similar to the younger monazite ages of the metasediments. This can be interpreted as evidence that titanite crystallized at the peak of regional metamorphism, as part of the reconstitution of the parent granitic rock to form an orthogneiss. The alternative explanation, that the titanite age reflects cooling below the closure temperature of titanite, is difficult to sustain in the light of the preservation of older titanite ages from amphibolite W403. The favored explanation is therefore that titanite crystallized close to the peak of regional metamorphism at ca. 2650 Ma.

Information on the post-peak temperature change can be obtained from the apatite results. Apatite ages from the orthogneiss W400 (2644 ± 19 Ma) and from the nearby syenite (2633 ± 6 Ma) (Pidgeon et al. 1996) are uncertain and may not be identical but nevertheless are younger than the titanites and are interpreted as cooling ages. Cherniak et al. (1991) proposed that the closure temperature of apatite falls within the range 550°C to 450°C for cooling rates of 1–10°C Ma^{-1} and crystal radii of 0.01 to 0.05 cm. These values are about 70°C lower than those reported by Watson et al. (1985). Nevertheless, on the basis of the size of apatites in the orthogneiss (0.01–0.05 cm), we favor a closure temperature of 500 ± 50°C from the results of Cherniak et al. (1991). Assuming an apatite closure age of ca. 2633 Ma and a T_c of 500°C, the temperature has dropped from 650–700°C at the peak of metamorphism at 2650 Ma to 500°C at about 2633 Ma, suggesting an average cooling rate of approximately 9 to 12°C Ma^{-1}.

The above ages relate to mineral growth and to the concept of closure temperature from Pb diffusion and form a basis for the construction of a temperature (T)-time (t) path that reflects the thermal equilibration between the different units. Thermal disequilibrium is frequently observed for plutonic

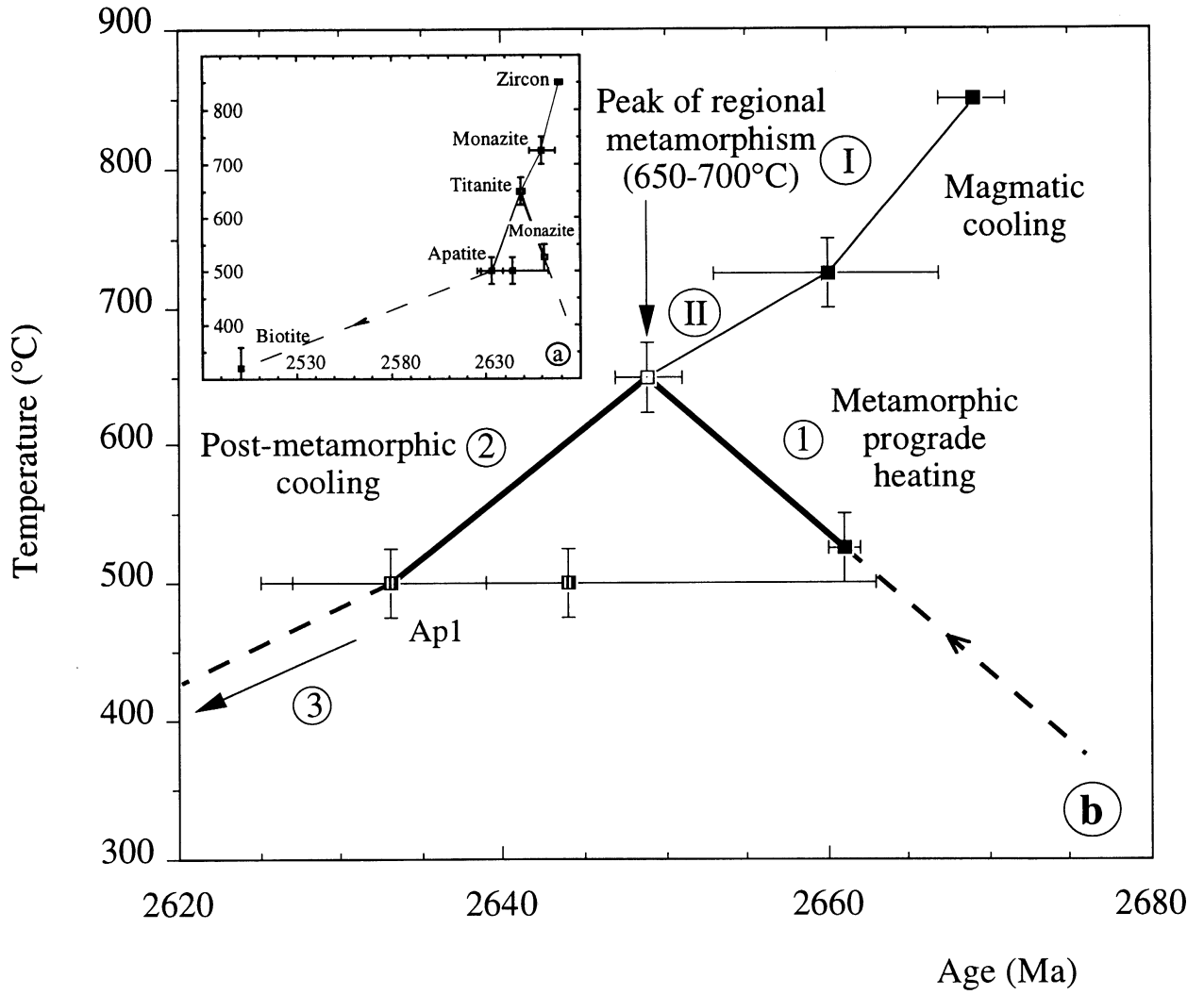

Figure 8. T-t path for accessory minerals analyzed from rocks from the Jimperding Metamorphic Belt in the Toodyay area. (*a*) All data; (*b*) expanded view of the period 2680–2620 Ma. Roman numbers refer to the average magmatic cooling history which involves equilibration with the country rocks and regional heating (I: -14°C Ma^{-1}, II: 5°C Ma^{-1}). Arab numbers and heavy line refer to the metamorphic prograde and retrograde history (1: $+12.5$°C Ma^{-1}, 2: -10°C Ma^{-1}, 3: -1.4°C Ma^{-1}). Estimated temperatures as follow: zircon, ca 850°C (from Watson and Harrison 1983 for I type granitic melt); monazite, 725 ± 25°C for the closure temperature (Copeland et al. 1988) and 525 ± 25°C for growth temperature in pelitic schists (Smith and Barreiro 1990); titanite, 650 ± 20°C for the closure temperature of 100–500 μm diffusion radii (Cherniak 1993); Apatite, 500 ± 25°C (Cherniak et al. 1991); Biotite (Rb-Sr), 320 ± 40°C (Harrison and McDougall 1980). Apatite age (Apl: 2633 ± 6 Ma) is from Pidgeon et al. (1996) Biotite age (ca. 2500 Ma) is from De Laeter and Libby (1993).

bodies and their country rocks and may also occur in heated metamorphic terranes where plutonic rocks are emplaced during different stages of metamorphism. This is probably enhanced by low-grade metamorphism, which is not capable of imposing its thermal signature on magmatic minerals and allows the magmatic bodies to remain at temperatures higher than those prevailing during the metamorphic climax. Figures 8*a* and *b* present a T-t path constructed on the basis of ages obtained in the present study. In figure 8*b*, Roman numbers illustrate the inferred average magmatic cooling history of the porphyritic granite, whereas Arab numbers and the heavy line represent the thermal metamorphic evolution. We relate the zircon age of sample W401 (2669 Ma) to crystallization in the magma at temperature of about 850°C (Watson and Harrison 1983). In the same way, the $^{207}Pb/^{206}Pb$ age of the monazite from the porphyritic granite is taken as reflecting cooling through the closure

temperature of this mineral rather than recrystallization or disturbances during metamorphism. Indeed, as pointed out above, metamorphism peaks at temperatures (650–700°C) under the closure temperature of the monazite (725 ± 25°C). Moreover, at ca. 2660 Ma it is likely that the magma was still hot, whereas country rocks were only at about 500°C. During this first stage, cooling of the plutonic bodies (from 850°C at 2669 Ma to 725°C at 2660 Ma) gives an average value of about $-14°CMa^{-1}$. The favored explanation that titanite from the orthogneiss W400 formed by recrystalization at 650°–700°C at peak metamorphic conditions allows to propose an average cooling rate of about $-5°C\ Ma^{-1}$ for the period 2650–2660 Ma. This model is consistent with cooling and progressive thermal equilibration of the magmatic body with the country rocks. The slight difference between the monazite closure temperature and the peak temperature conditions suggests that a thermal equilibration between the different units of the belt has been reached at about 2650 Ma. The 2661 Ma monazite age in the metasediments dates crystallization of this mineral during prograde metamorphism at about 525°C. The 2652 Ma age for some monazites, zircons from the Katrine syenite (Pidgeon et al. 1996), and titanite from the orthogneiss, is consistent with a pattern of increasing temperature to a metamorphic climax at about 650–700°C at this age, and we suggest an average heating rate of ca $+ 15°C\ Ma^{-1}$ from 2660 Ma to 2650 Ma. This is comparable with the heating rate for Palaeozoic events such as the Alpine orogen in the Central Swiss Alps (Vance and O'Nions 1992) or the Caledonian orogen in Norway (Burton and O'Nions 1991). After peak metamorphism, the temperature gradually decreased to reach the blocking temperature of apatite at 2644 ± 19 Ma or at the more precise 2633 ± 6 Ma age from the Katrine syenite apatite (Pidgeon et al. 1996) with an approximate cooling rate of ca $-10°C\ Ma^{-1}$. De Laeter and Libby (1993) reported Rb/Sr analyses on biotite from throughout the southwestern part of the Yilgarn Craton and, except in the vicinity of the Darling Fault where ages have been reset, biotites yield ages of about 2500 Ma, which can be related to cooling below the Sr closure temperature of biotite (figure 8). Combined with the 2633 ± 6 Ma U-Pb age of apatite from the Katrine syenite (Pidgeon et al. 1996), the cooling rate during the interval 2500–2630 Ma is ca. $-1.4°C\ Ma^{-1}$. Such a cooling rate could be produced by isostatic recovery and very low erosion rate.

Implications for the Evolution of the Southwestern Margin of the Yilgarn Craton. The present results define a period of granite emplacement, deformation and metamorphism followed by cooling which took place during about 35 m.y., from ca. 2670 Ma to about 2635 Ma. The chain of events began with emplacement of early granitoids in the period 2670–2660 Ma during deformation and metamorphism, which increased in intensity, reaching a climax at about 2650 Ma. This prograde period was accompanied by the formation of migmatites, the deformation and melting of early granitoids, and the intrusion and metamorphism of ultramafic magmas. Titanites were crystallized or recrystallized and some monazite grains were updated at 2650 Ma, corresponding to the metamorphic climax, and confirming the age of regional granulite facies metamorphism, dated at between 2640 and 2650 Ma by Nemchin et al. (1994). Granite emplacement continued for a short period after the waning of tectonic activity. The final event of this episode was the emplacement of swarms of aplite and pegmatite dikes into the belt and the granites themselves. This period of tectonism and igneous emplacement may represent a major episode of plate tectonic activity, as suggested by Myers (1990), which swept together and amalgamated a number of diverse crustal fragments. This is supported by gravity and seismic data that suggests that a NNW line through the JMB in the vicinity of Toodyay marks a fundamental change in crustal structure (Fraser and Pettifer 1980). Whereas gravity increases relatively west of this line, known as the Yandanooka-Cape Riche lineament, seismic studies have shown that crustal thickness is also greater to the west of the lineament (Mathur 1974). These relationships are compatible with the interpretation that the JMB represents the foreland of a collisional belt. The present study indicates that the tectonic/metamorphic episode (i.e., from 500°C in the prograde stage to 500°C in the retrograde stage) is about 30 m.y. and that this period was subsequently followed by gradual cooling. This is not compatible with underplating phenomena, which typically lasts longer, up to 100 m.y. (Krogh 1993; Bolhen and Mezger 1989). Alternatively, the episode of tectonism, plutonism, and metamorphism was more likely due to crustal thickening caused by nappe stacking and responsible for partial melting and granite emplacement as a result of the collision of tectonic plates at ca. 2670 Ma.

Conclusions

The JMB formed as a series of shelf sediments in the middle Archean and was subjected to a major episode of tectonism, plutonism, and high-grade

metamorphism within a narrow span of time from 2670 to 2635 Ma. This episode shows a sequence of events from early emplacement of granitic plutons through increasing deformation and metamorphism, reaching a temperature peak at 2650 Ma, followed by cooling. The impact of this episode is widespread in the southwest Yilgarn Craton and represents the final Late-Archean craton-forming event of the Yilgarn. The timing of events within this episode has been established by combining the U-Pb dating of minerals with a knowledge of their characteristic temperatures of formation and their closure temperatures to Pb diffusion.

1) SHRIMP U-Pb analyses of detrital zircons show that the deposition of clastic sediments took place during the interval 3055–2700 Ma, possibly on a basement constituted by ca. 3.25 Ga old rocks, and may have been contemporaneous with sedimentation of the Jack Hills Supracrustal association. Although similar in age (Archean to Early Archean), the sedimentary source rocks were probably different.

2) Emplacement of granitic plutons occurred during the prograde stage of metamorphism (2660–2670 Ma). The main metamorphic monazite generation crystallized at ca. 2661 Ma as the temperature reached ca. 525°C during the prograde metamorphism of the pelitic schists.

3) Peak regional amphibolite facies metamorphism occurred at ca. 2650 Ma and may have been responsible for the growth of titanite in the orthogneiss W400. Farther east, this period culminated in high-grade metamorphism, reaching HP-LT granulite facies conditions. Average prograde heating rate was ca 15°C Ma^{-1} and rocks were subsequently cooled slowly (from ca 10 to 1–2°C Ma^{-1}) by processes consistent with isostatic recovery and erosion.

4) A mechanism of continental collision and crustal thickening by nappe stacking is proposed as the best explanation for the late Archean tectonic episode affecting the Jimperding Belt.

ACKNOWLEDGMENTS

This study has been realized in the laboratory of R.T. Pidgeon at the Curtin University of Technology, supported by the Australian Research Council, during the research fellowships of two of us (D.B. and O.B.). D.B. acknowledges support from the CNRS. O.B. was supported by an ARC international fellowship. The paper greatly benefited for the constructive reviews by C.R.L Friend, W. Todt, and one anonymous reviewer. Special thanks to D. Byrne for his help with the mineralogical examination of the thin sections and for our friendly relationship. Helpful advises from A. Kennedy, P. Kinny, and A. Nemchin while running the SHRIMP II were greatly appreciated.

REFERENCES CITED

Arriens, P. A., 1971, The Archean geochronology of Australia: Geol Soc. Australia Spec. Pub. v. 3, p. 11–23.

Black, L. P., 1987, Recent Pb loss in zircon: A natural or laboratory-induced phenomenon?: Chem. Geol., v. 65, p. 25–33.

———; Fitzgerald, J. D.; and Harley, S. L., 1984, Pb isotopic composition, color, and microstructure of monazites from a polymetamorphic rock in Antarctica: Contrib. Mineral. Petrol., v. 85, p. 141–148.

Bolhen, S. R., and Mezger, K., 1989. Origin of granulite terranes and the formation of the lowermost continental crust: Science, v. 244, p. 326–329.

Burton, K. W., and O'Nions, R. K., 1991, High-resolution garnet chronometry and the rates of metamorphic processes: Earth Planet, Sci. Lett., v. 107, p. 649–671.

Cherniak, D. J., 1993, Lead diffusion in titanite and preliminary results on the effects of radiation damage on Pb transport: Chem. Geol., v. 110, p. 177–194.

———; Lanford, W. A.; and Ryerson, F. J., 1991, Lead diffusion in apatite and zircon using ion implantation and Rutherford backscattering techniques: Geochim. Cosmochim. Acta, v. 55, p. 1663–1673.

Compston, W., and Pidgeon, R. T., 1986, Jack Hills evidence of more very old detrital zircons in Western Australia: Nature, v. 321, p. 766–769.

———; Williams, I. S.; and Meyer, C., 1984, U-Pb geochronology of zircons from lunar breccia 73217 using a sensitive high-resolution ion-microprobe, *in* Proc., 14th Lunar Sci. Conf.: Jour. Geophys. Res., v. 89, p. 525–534.

Copeland, P.; Parrish, R. R.; and Harrison, T. M., 1988, Identification of inherited radiogenic Pb in monazite and its implications for U-Pb systematics: Nature, v. 333, p. 760–763.

Corfu, F., 1988, Differential response of U-Pb systems in coexisting accessory minerals, Winnipeg River Subprovince, Canadian Shield: implications for Archean crustal growth and stabilization: Contrib. Mineral. Petrol., v. 98, p. 312–325.

De Laeter, J. R., and Libby, W. G., 1993, Early Palaeozoic biotite Rb-Sr dates in the Yilgarn Craton near Harvey, Western Australia: Austral. Jour. Earth Sci., v. 40, p. 445–453.

De Wolf, C. P.; Belshaw, N.; and O'Nions, R. K., 1993,

A metamorphic history from micro-scale $^{207}Pb/^{206}Pb$ chronometry of Archean monazite: Earth Planet. Sci. Lett., v. 120, p. 207–220.

Fraser, A. R., and Pettifer, G. R., 1980. Reconnaissance gravity surveys in W.A. and S.A., 1969–1972: Bur. Min. Res. Bull. 196, 60 p.

Gee, R. D.; Baxter, S. A.; Wilde, S. A.; and Williams, I. R., 1981. Crustal development in the Archean Yilgarn Block, Western Australia, *in* Glover, J. E., and Groves, D. I., eds., Archean geology, Second Int. Symp. (Perth 1980): Geol. Soc. Australia Spec. Publ. 7, p. 43–57.

Goldich, S. S., and Mudrey, J. R., 1972, Dilatancy model for discordant U-Pb zircon ages: Contrib. to Recent Geochemistry and Analytical Chemistry (Vinogradov volume): Moscow, Nauka. Publ. Office, p. 415–418.

Harrison, T. M., and McDougall, 1980, Investigations of an intrusive contact, northwest Nelson, New Zealand. II. Thermal, chronological, and isotopic constraints: Geochim. Cosmochim. Acta, v. 44, p. 1985–2003.

Jaffey, A. H.; Flynn, D. F.; Glendenin, L. E.; Bentlye, W. C.; and Essling, A. M., 1971, Precision measurement of the half-lives and specific activities of ^{235}U and ^{238}U: Phys. Rev., v. 4 (c), p. 1889–1906.

Kingsbury, J. A.; Miller, C. F. M.; Wooden, J. L.; and Harrison, H. M., 1993, Monazite paragenesis and U-Pb systematics in rocks of the eastern Mojave desert, California, USA: Implications for thermochronometry; Chem. Geol., v. 1190, p. 147–167.

Kinny, P. D., 1990, Age spectrum of detrital zircons in the Windmill Hill Quartzite, *in* Ho, S. E.; Glover, J. E.; Myers, J. S.; and Mulhing, J. R., eds., Third International Archean Symposium, Excursion Guidebook, Excursion N. 4, Toodyay-Chittering, p. 213–218.

———; Wijbrans, J. R.; Froude, D. O.; Williams, I. S.; and Compston, W., 1990, Age constraints on the geological evolution of the Narryer Gneiss Complex, Western Australia: Austral. Jour. Earth. Sci., v. 37, p. 51–69.

Krogh, T. E., 1973, A low-contamination method for hydrothermal decomposition of zircon and extraction of U and Pb for isotopic age determinations: Geochim. Cosmochim. Acta, v. 37, p. 485–494.

———; 1982, Improved accuracy of U-Pb zircon ages by the creation of more concordant systems using an air abrasion technique: Geochim. Cosmochim. Acta, v. 46, p. 637–649.

———; 1993, High precision U-Pb ages for granulite metamorphism and deformation in the Archean Kapuskasing structural zone, Ontario: Implications for structure and development of the lower crust: Earth Planet. Sci. Lett., v. 119, p. 1–18.

Ludwig, K. R., 1987, Isoplot200, a plotting and regression program for isotope geochemists, for use with HP series 200 computers: U.S. Geol. Survey Open File Rept. 85-513, 38 p.

Manhes, G.; Minster, J. F.; and Allegre, C. J., 1978, Comparative Uranium-Thorium-Lead and Rubidium-Strontium study in Saint-Severin amphoterite—Consequences on early solar system chronology: Earth Planet. Sci. Lett., v. 39, p. 14–24.

Mathur, S. P., 1974, Crustal structure in southwestern Australia from seismic and gravity data: Tectonophysics, v. 24, p. 151–182.

Myers, J. S., 1990, Precambrian tectonic evolution of part of Gondwana, southwestern Australia: Geology, v. 18, p. 537–540.

Nemchin, A. A.; Pidgeon, R. T.; and Wilde, S. A., 1994, Timing of Late Archean granulite facies metamorphism in the southwestern Yilgarn Craton of Western Australia: Evidence from U-Pb ages of zircons from mafic granulites: Precamb. Res., v. 68, p. 307–321.

Nieuwland, D. A., and Compston, W., 1981, Crustal evolution in the Yilgarn block near Perth, Western Australia, *in* Glover J. E., and Groves, D. I., eds., Archean geology, Second Int. Symp. (Perth 1980); Geol. Soc. Australia, Spec. Pub. 7, p. 159–171.

Nutman, A. P.; Kinny, P. K.; Compston, W.; and Williams, I. S., 1991, SHRIMP U-Pb zircon geochronology of the Narryer Gneiss Complex, Western Australia: Precamb. Res., v. 52, p. 275–300.

Parrish, R. R., 1987, An improved micro-capsule for zircon dissolution in U-Pb geochronology: Chem. Geol., v. 66, p. 99–102.

———; 1990, U-Pb dating of monazite and its application to geological problems: Can. Jour. Earth. Sci., v. 27, p. 1431–1450.

———; and Tirrul, R., 1989, U-Pb age of the Baltoro granite, northwest Himalaya, and its implications for monazite U-Pb systematics: Geology, v. 17, p. 1076–1079.

Pidgeon, R. T.; Bosch, D.; and Bruguier, O., 1996, Petrogenetic implications of inherited zircon and titanite in the Archean Katrine syenite, southwestern Yilgarn Craton, Western Australia: Earth Planet. Sci. Lett., v. 141, p. 187–198.

———; Furfaro, D.; Kennedy, A. K.; Nemchin, A. A.; and Van Bronswjk, W., 1994, Calibration of zircon standards for the Curtin SHRIMP II: Eight International Conference on Geochronology, Cosmochronology and Isotope Geology (Berkeley); Abs. vol., U.S. Geol. Survey Cir. 1107, p. 251.

Scharer, U.; Krogh, T. E.; and Glower, C. F., 1986, Age and evolution of the Grenville province in eastern Labrador from U-Pb systematics in accessory minerals: Contrib. Mineral. Petrol., v. 94, p. 438–451.

Smith, H. A., and Barreiro, B., 1990, Monazite U-Pb dating of staurolite grade metamorphism in pelitic schists: Contrib. Mineral. Petrol., v. 105, p. 602–615.

Stacey, J. S., and Kramers, J. D., 1975, Approximation of terrestrial lead isotope evolution by a two-stage model: Earth Planet, Sci. Lett., v. 6, p. 15–25.

Steiger, R. H., and Jäger, E., 1977, Subcommission on Geochronology: Convention in the use of decay constants in geo- and cosmochronology: Earth Planet Sci. Lett., v. 36, p. 359–362.

Stern, T. W.; Goldich, S. S.; and Newell, M. F., 1966,

Effects of weather on the U-Pb ages of zircon from the Morton gneiss. Minnesota: Earth Planet. Sci. Lett., v. 1, p. 369–371.

Tucker, R. D.; Raheim, A.; Krogh, T. E.; and Corfu, F., 1987, Uranium-lead zircon and titanite ages from the northern portion of the Western Gneiss Region, south central Norway: Earth. Planet. Sci. Lett., v. 81, p. 203–211.

Vance, D., and O'Nions, R. K., 1992, Prograde and retrograde thermal histories from the central Swiss Alps: Earth Planet. Sci. Lett., v. 114, p. 113–129.

Watson, E. B., and Harrison, T. M., 1983, Zircon saturation revisited: temperature and composition effects in a variety of crustal magma types: Earth Planet. Sci. Lett., v. 64, p. 295–304.

———; ———; and Ryerson, F. J., 1985, Diffusion of Sm, Sr and Pb in fluorapatite: Geochim. Cosmochim. Acta, v. 49, p. 1813–1823.

Williams, I. S.; Compston, W.; Black, L. P.; Ireland, T. R.; and Foster, J. J., 1984, Unsupported radiogenic Pb in zircon: A cause of anomalously high Pb-Pb, U-Pb, and Th-Pb ages: Contrib. Mineral. Petrol., v. 88, p. 322–327.

Wilde, S. A., 1980, The Jimperding Metamorphic Belt in the Toodyay area and the Ballingup Metamorphic Belt and associated granitic rocks of the southwestern Yilgarn Block, *in* Second Int. Archean Symp. (Perth 1980), Excursion Guide: Perth, Geol. Soc. Australia, 41p.

———; and Low, G. H., 1978, Perth, Western Australia: Western Australian Geological Survey 1:250,000 Geological Series Explanatory Notes, 36 p.